ELSEVIER

Sedimentary Geology 128 (1999) 155–169

Sedimentary Geology

Depositional style and subsidence history of the Turpan Basin (NW China)

Lei Shao [a,b,*], Karl Stattegger [b], Wenhou Li [c], Bernd J. Haupt [b,d]

[a] *Laboratory of Marine Geology, Tongji University, Shanghai 200092, P.R. China*
[b] *Institute of Geoscience, University of Kiel, Kiel, Germany*
[c] *Department of Geology, Northwest University, Xi'an 710069, P.R. China*
[d] *Earth System Science Center, Pennsylvania State University, University Park, PA, USA*

Received 17 February 1998; accepted 5 May 1999

Abstract

The Turpan Basin has a complex polycyclic sedimentary and tectonic history from Late Permian to late Tertiary time. Main stratigraphic boundaries are unconformities that bound tectonically induced sedimentary cycles. The depositional style reflects a continental environment exhibiting changes from alluvial fan/fluvial to lacustrine conditions within each cycle. More than 7000 m of clastic sediments accumulated during the evolution of the basin. Paleocurrent analysis reveals a complex pattern of sediment dispersal pathways into the basin. On the southern margin of the basin, the transport direction is always directed from south to north indicating sediment sources in the Jueluotage Shan, while in the northern part the Late Jurassic uplift of the Bogda Shan provided an important source area from the Early Cretaceous onwards with transport directions from north to south. After basin formation during the Late Permian, the Turpan Basin underwent first thermal subsidence and then flexural subsidence. The thermal subsidence took place during the Late Permian and Early Triassic following the period of magmatic activities in this region. The flexural subsidence was throughout the Middle Triassic to early Tertiary induced by collisions and accretions onto the south Asian continental margin of the Qiangtang Block in the Late Triassic/Early Jurassic, the Gangdise Block in latest Jurassic/earliest Cretaceous, and the Indian Subcontinent in the latest Cretaceous/early Cenozoic.

Keywords: basin analysis; NW China; sedimentology; subsidence; Turpan Basin

1. Introduction

The Turpan Basin, located in northwest China (42º–43º30′N; 87º30′–95º30′E), is a relatively large intermontane basin of the Tian Shan (Shan is the Chinese term for mountain). This basin is approximately 500 km long from east to west, 60–100 km wide from south to north, and covers an area of 53,500 km^2. The Turpan Basin is connected to the north and northeast with the Bogda Shan and Haerlike Shan and towards the south with the Jueluotage Shan, adjacent to the Tarim Basin (Fig. 1). Most of the basin consists of desert. The Aiding Lake, located in the southwest of the basin, lies at an altitude of 154 m below sea level and is the second lowest continental point in the world.

The Turpan Basin has been intensively studied

* Corresponding author. Fax: +86 21659 88808; E-mail: lshaok@online.sh.cn

0037-0738/99/$ – see front matter
PII: S0037-0738(99)00066-4

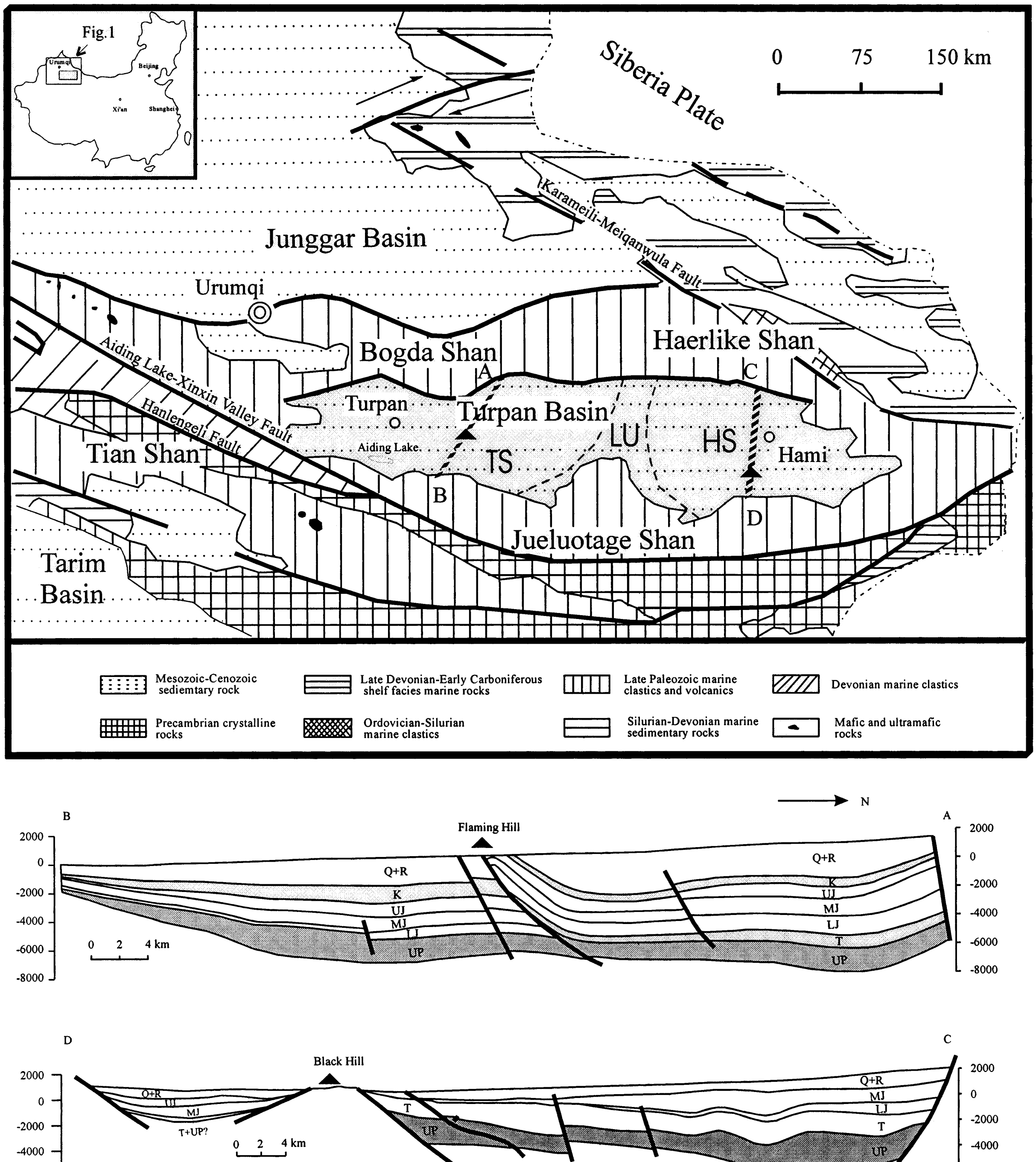

Fig. 1. Geologic map of northwest China (after Chen, 1985a) and two cross-sections. This map shows only the distribution of pre-Mesozoic rocks. *TS* = Turpan Sag; *LU* = Ledong Uplift; *HS* = Hami Sag.

since the 1980s, after the discovery of oil fields (Wu and Zhao, 1997); nevertheless, published geological studies remain sparse. Differing views exist on the timing and development of the Turpan Basin, its tectonic setting, its basement and its tectonic evolution. Some authors have proposed that the Tian Shan is strictly a manifestation of the Cenozoic Himalayan orogeny (Bally et al., 1986). Others suggest that the Tian Shan area including the Junggar, Turpan and Tarim basins, has a long and polycyclic tectonic history (Huang, 1978; Ren et al., 1980; Zhu and Chen, 1980; Zhang and Wu, 1985; Zhu and Yang, 1988; Carroll et al., 1991; Hendrix et al., 1992; Allen and Windley, 1993; Peng et al., 1995). Some studies consider that the Turpan Basin is a late Paleozoic intermontane basin of the Tian Shan orogenic belt (Cao, 1990). However, other studies maintain that the Turpan Basin is a microcontinent, which was connected to the Junggar Basin prior to Late Permian time (Q. Wu, 1986; Z. Wu, 1986; Tang and Zhao, 1991; Lin, 1993; Hu et al., 1996). On the basis of the outcrop of Precambrian crystalline rock in the surrounding orogenic belts of the Junggar and Turpan basins and geophysical data, the Turpan and Junggar basins are considered as having a Precambrian crystalline basement and belonging to the Eurasia Plate (Q. Wu, 1986; T. Wu et al., 1992, 1996; Zhao et al., 1992; Xiao et al., 1992). Another view is that the Turpan Basin and Junggar Basin developed on an oceanic crust based on sedimentary sequence and volcanics (Carroll et al., 1990, 1991). Clearly, the controversy and differing views about this region have arisen from a lack of detailed geological data.

2. Geological background

The Turpan Basin is located in the eastern part of the Tian Shan, which is a distal portion of the Himalayan orogenic belts formed by the collision between the Indian and Eurasian plates in the Cenozoic. The Bogda Shan consists of Upper Carboniferous, Permian, Triassic and some Jurassic rocks. The Late Carboniferous is dominated by volcaniclastic and carbonate strata of mainly neritic or continental facies, with some interbedded intermediate and intermediate–felsic volcanic rocks. There is minor diabase and gabbro intrusive rock outcropping in the core of the mountains (Chen, 1985a). The Permian is represented by continental clastic–pyroclastic formations and minor limestone. The Triassic, Lower and Middle Jurassic consist of continental clastic formations with coal seams. The Carboniferous and Permian show very low-grade or no metamorphism. In comparison, the Haerlike Shan adjacent to the Bogda Shan in the east contains Devonian and Lower Carboniferous clastic–pyroclastic strata of neritic facies and intermediate, intermediate–felsic and felsic volcanic rocks, which were more affected by regional metamorphism and granite plutonism than in the Bogda Shan. The Triassic and Jurassic are absent in the Haerlike Shan. Some studies maintain that the Bogda Shan was together with the Haerlike Shan a continental rift valley based on volcanic geochemical data in the Carboniferous and Early Permian (Lin, 1993; He et al., 1994; Zhou et al., 1996). The Jueluotage Shan, located south of the Turpan Basin, consists of Silurian, Devonian and Carboniferous metamorphosed felsic and intermediate–felsic volcanic, pyroclastic formations, and marine sedimentary, ultramafic, mafic and intermediate–felsic plutonic complexes. In Late Carboniferous and Permian time, a great many felsic and intermediate–felsic plutons (mainly of granite, biotite granite and alkali–granite, and minor granodiorite and diorite) intruded this region (Chen, 1985b).

The basement of the Turpan Basin was deformed by Paleozoic tectonism (Zhao et al., 1992). Due to the collision between the Indian and Eurasian plates in the Cenozoic, this basin was redeformed and as a result a north to south (W–E elongated) thrust fault belt formed in the middle of the basin (Flaming Hills, see Fig. 1, cross-section). The Turpan Basin can be subdivided into three regions (Fig. 1): Turpan Sag, Ledong Uplift and Hami Sag (Zhao et al., 1992). There are only some Lower and Middle Jurassic sedimentary cover sequences in the Ledong Uplift, and Late Permian to Cenozoic sedimentary cover sequences in the Turpan Sag and Hami Sag.

3. Materials and methods

This paper is based on a detailed study of outcrop sections in field and core logs, and backstripping analysis of the stratigraphic data. Twenty-two sec-

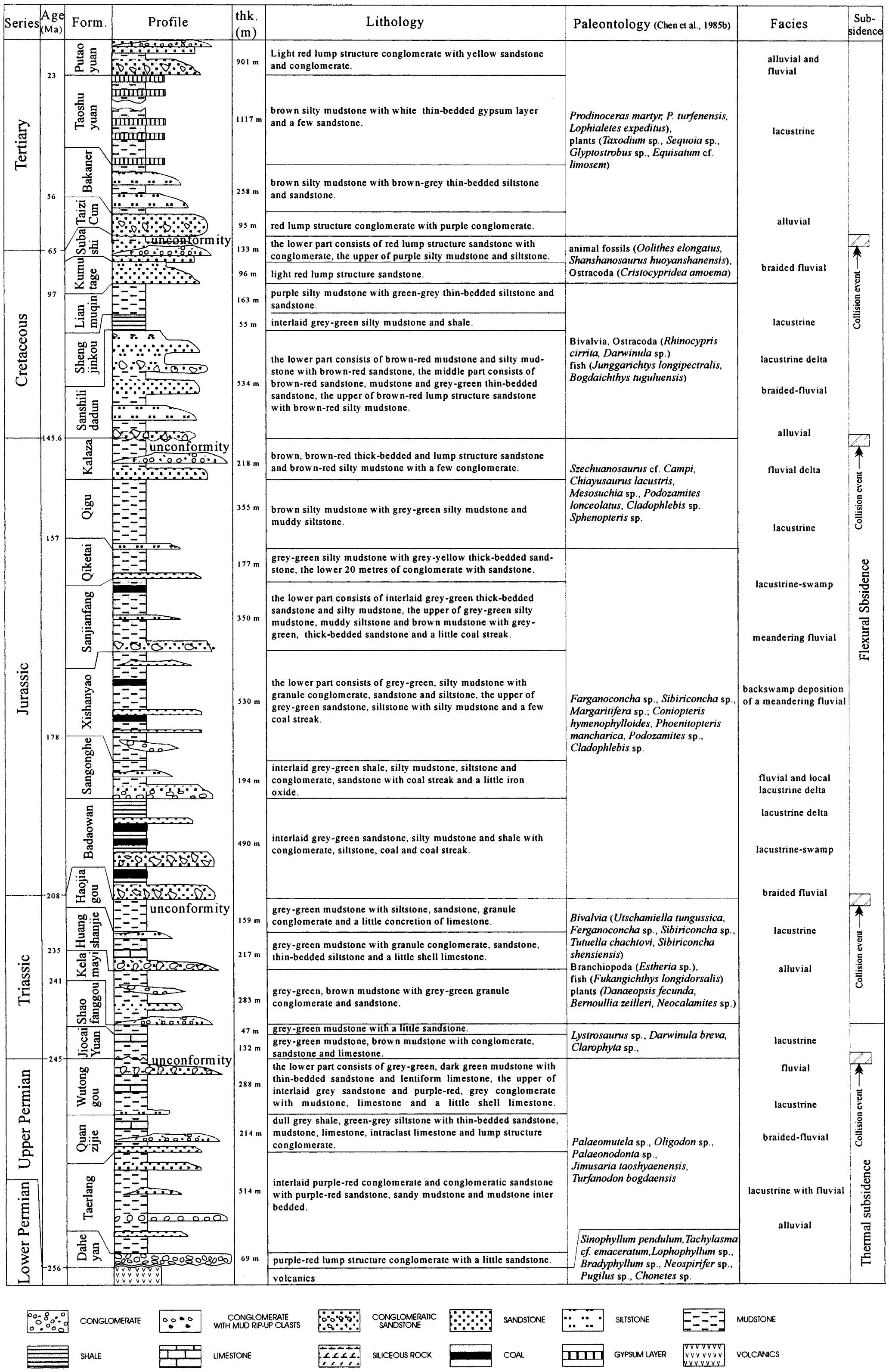
Series
Age (Ma)
Form.
Profile
thk. (m)
Lithology
Paleontology (Chen et al., 1985b)
Facies
Sub-sidence
Tertiary
23
56
65
Putao yuan
901 m
Light red lump structure conglomerate with yellow sandstone and conglomerate.
alluvial and fluvial
Taoshu yuan
1117 m
brown silty mudstone with white thin-bedded gypsum layer and a few sandstone.
Prodinoceras martyr, P. turfenensis, Lophialetes expeditus), plants (Taxodium sp., Sequoia sp., Glyptostrobus sp., Equisatum cf. limosem)
lacustrine
Bakaner
258 m
brown silty mudstone with brown-grey thin-bedded siltstone and sandstone.
Taizi Cun
95 m
red lump structure conglomerate with purple conglomerate.
alluvial
unconformity
Subashi
133 m
the lower part consists of red lump structure sandstone with conglomerate, the upper of purple silty mudstone and siltstone.
animal fossils (Oolithes elongatus, Shanshanosaurus huoyanshanensis), Ostracoda (Cristocypridea amoema)
braided fluvial
Cretaceous
97
145.6
Kumutage
96 m
light red lump structure sandstone.
Lianmuqin
163 m
purple silty mudstone with green-grey thin-bedded siltstone and sandstone.
55 m
interlaid grey-green silty mudstone and shale.
lacustrine
Shengjinkou
Sanshilidadun
534 m
the lower part consists of brown-red mudstone and silty mudstone with brown-red sandstone, the middle part consists of brown-red sandstone, mudstone and grey-green thin-bedded sandstone, the upper of brown-red lump structure sandstone with brown-red silty mudstone.
Bivalvia, Ostracoda (Rhinocypris cirrita, Darwinula sp.) fish (Junggarichtys longipectralis, Bogdaichthys tuguluensis)
lacustrine delta
braided-fluvial
alluvial
Collision event
unconformity
Jurassic
157
178
208
Kalaza
218 m
brown, brown-red thick-bedded and lump structure sandstone and brown-red silty mudstone with a few conglomerate.
Szechuanosaurus cf. Campi, Chiayusaurus lacustris, Mesosuchia sp., Podozamites lonceolatus, Cladophlebis sp. Sphenopteris sp.
fluvial delta
Qigu
355 m
brown silty mudstone with grey-green silty mudstone and muddy siltstone.
lacustrine
Collision event
Qiketai
177 m
grey-green silty mudstone with grey-yellow thick-bedded sandstone, the lower 20 metres of conglomerate with sandstone.
lacustrine-swamp
Sanjianfang
350 m
the lower part consists of interlaid grey-green thick-bedded sandstone and silty mudstone, the upper of grey-green silty mudstone, muddy siltstone and brown mudstone with grey-green, thick-bedded sandstone and a little coal streak.
meandering fluvial
Flexural Sbsidence
Xishanyao
530 m
the lower part consists of grey-green, silty mudstone with granule conglomerate, sandstone and siltstone, the upper of grey-green sandstone, siltstone with silty mudstone and a few coal streak.
Farganoconcha sp., Sibiriconcha sp., Margaritifera sp.; Coniopteris hymenophylloides, Phoenitopteris mancharica, Podozamites sp., Cladophlebis sp.
backswamp deposition of a meandering fluvial
Sangonghe
194 m
interlaid grey-green shale, silty mudstone, siltstone and conglomerate, sandstone with coal streak and a little iron oxide.
fluvial and local lacustrine delta
Badaowan
490 m
interlaid grey-green sandstone, silty mudstone and shale with conglomerate, siltstone, coal and coal streak.
lacustrine delta
lacustrine-swamp
Haojiagou
braided fluvial
unconformity
Triassic
235
241
245
Huangshanjie
159 m
grey-green mudstone with siltstone, sandstone, granule conglomerate and a little concretion of limestone.
Bivalvia (Utschamiella tungussica, Ferganoconcha sp., Sibiriconcha sp., Tutuella chachtovi, Sibiriconcha shensiensis) Branchiopoda (Estheria sp.), fish (Fukangichthys longidorsalis) plants (Danaeopsis fecunda, Bernoullia zeilleri, Neocalamites sp.)
lacustrine
Kelamayi
217 m
grey-green mudstone with granule conglomerate, sandstone, thin-bedded siltstone and a little shell limestone.
alluvial
Collision event
Shaofanggou
283 m
grey-green, brown mudstone with grey-green granule conglomerate and sandstone.
47 m
grey-green mudstone with a little sandstone.
Jiocaiyuan
132 m
grey-green mudstone, brown mudstone with conglomerate, sandstone and limestone.
Lystrosaurus sp., Darwinula breva, Clarophyta sp.,
lacustrine
unconformity
Upper Permian
Wutonggou
288 m
the lower part consists of grey-green, dark green mudstone with thin-bedded sandstone and lentiform limestone, the upper of interlaid grey sandstone and purple-red, grey conglomerate with mudstone, limestone and a little shell limestone.
fluvial
lacustrine
Quanzijie
214 m
dull grey shale, green-grey siltstone with thin-bedded sandstone, mudstone, limestone, intraclast limestone and lump structure conglomerate.
Palaeomutela sp., Oligodon sp., Palaeonodonta sp., Jimusaria taoshyaenensis, Turfanodon bogdaensis
braided-fluvial
Collision event
Taerlang
514 m
interlaid purple-red conglomerate and conglomeratic sandstone with purple-red sandstone, sandy mudstone and mudstone inter bedded.
lacustrine with fluvial
alluvial
Thermal subsidence
Lower Permian
256
Daheyan
69 m
purple-red lump structure conglomerate with a little sandstone.
Sinophyllum pendulum, Tachylasma cf. emaceratum, Lophophyllum sp., Bradyphyllum sp., Neospirifer sp., Pugilus sp., Chonetes sp.
volcanics
CONGLOMERATE
CONGLOMERATE WITH MUD RIP-UP CLASTS
CONGLOMERATIC SANDSTONE
SANDSTONE
SILTSTONE
MUDSTONE
SHALE
LIMESTONE
SILICEOUS ROCK
COAL
GYPSUM LAYER
VOLCANICS

tions in the western Turpan Sag and the eastern Hami Sag of the Turpan Basin were examined. Fifteen sections and seven core profiles ranging from the Carboniferous to the Tertiary were surveyed. The comprehensive stratigraphic section of the northern part of the basin is shown in Fig. 2 and locations of all surveyed sections are shown in Fig. 3. A total of 930 paleocurrent measurements from the Triassic to the Jurassic strata were made and collected (124 for the Triassic and 806 for the Jurassic). Potter and Pettijohn (1963) and Miall (1990) described the directional character of sedimentary rock and the method of measurement. In this study, current directions have been measured with a compass. Linear structures (sole markings, parting lineation), ripples, trough crossbedding and planar crossbedding were used. The subsidence history derived from the stratigraphic data of the northern part of the Turpan Sag is used to evaluate models for sedimentary basin evolution. We used the backstripping method of van Hinte (1978) and Steckler and Watts (1978). The absolute ages are based on Harland et al. (1990). The purpose of this paper is to interpret the evolutionary history of the Turpan Basin. Results on sandstone petrology and geochemistry are outlined in Shao (1996) and Shao et al., 1999).

4. Stratigraphy

Although some of the stratigraphic relationships in the basin have been studied in the fifties and sixties (Bureau of Geology and Mineral Resources of Xinjiang Uygur Autonomous Region, 1966) and some petrological investigations were carried out on various rock collections, no rigorous stratigraphic scheme was established before the eighties. Since 1980, increased field activity by the Bureau of Geology and Mineral Resources of Xinjiang Uygur Autonomous Region and the Bureau of Oil and Gas Management of Yumen has yielded new geological information. A system of nomenclature and a stratigraphic scheme has been established for the whole basin (Zhang, 1981; Zhang, 1983; Chen, 1985b). This stratigraphic scheme, based both on biostratigraphic and petrographic data, is widely used. The thickness of sedimentary strata in the basin is variable. Fig. 2 shows the stratigraphy and thickness of sedimentary formations in the northern part of the Turpan Sag, where strata are thickest. Figs. 3 and 4 show the two most extensive outcrop-sections (the Taoshuyuan and Lianmuqin sections).

The sediment fill of the Turpan Basin contains more than 7000 m of continental sediments of Late Permian to late Tertiary age. Upper Carboniferous and Lower Permian volcanics, clastics and platform carbonates are known from neighboring areas and extend into the margins of the Turpan Basin. The sedimentary environments of Upper Carboniferous and Lower Permian age were studied (Jin and Li, 1989; Jin, 1989; Song and Jin, 1989; Bureau of Geology and Mineral Resources of Xinjiang Uygur Autonomous Region, 1991; Wu and Zhao, 1997). During the Permian the sedimentary environment shifted from marine to fluvial and lacustrine conditions and the Turpan Basin became an individual depocenter from the Late Permian onwards (Zhu and Yang, 1988; Wu and Zhao, 1997). These terrestrial conditions prevailed also during Mesozoic and Cenozoic times.

5. Depositional style of basin fill

The Turpan Basin has a complex polycyclic sedimentary and tectonic history. The main stratigraphic boundaries follow in general tectonically induced sedimentary cycles, which are bounded by unconformities. The depositional style reflects a continental environment exhibiting changes from alluvial fan/fluvial to lacustrine conditions within each cycle.

Upper Permian strata in the Turpan Basin are mostly nonmarine. The middle of the basin received lacustrine deposits. At the northern and western margins of the basin, the basal part of the strata consists of rapid alluvial and fluvial conglomerates, which are directly derived from the underlying strata. Most part of the Bogda Shan was at that time a sedimentary basin. The transport direction of the sediments in the northern Turpan Basin and at Taoshuyuan was from southwest to northeast (Carroll et al., 1991).

Fig. 2. The comprehensive composite stratigraphic section of the Turpan Basin.

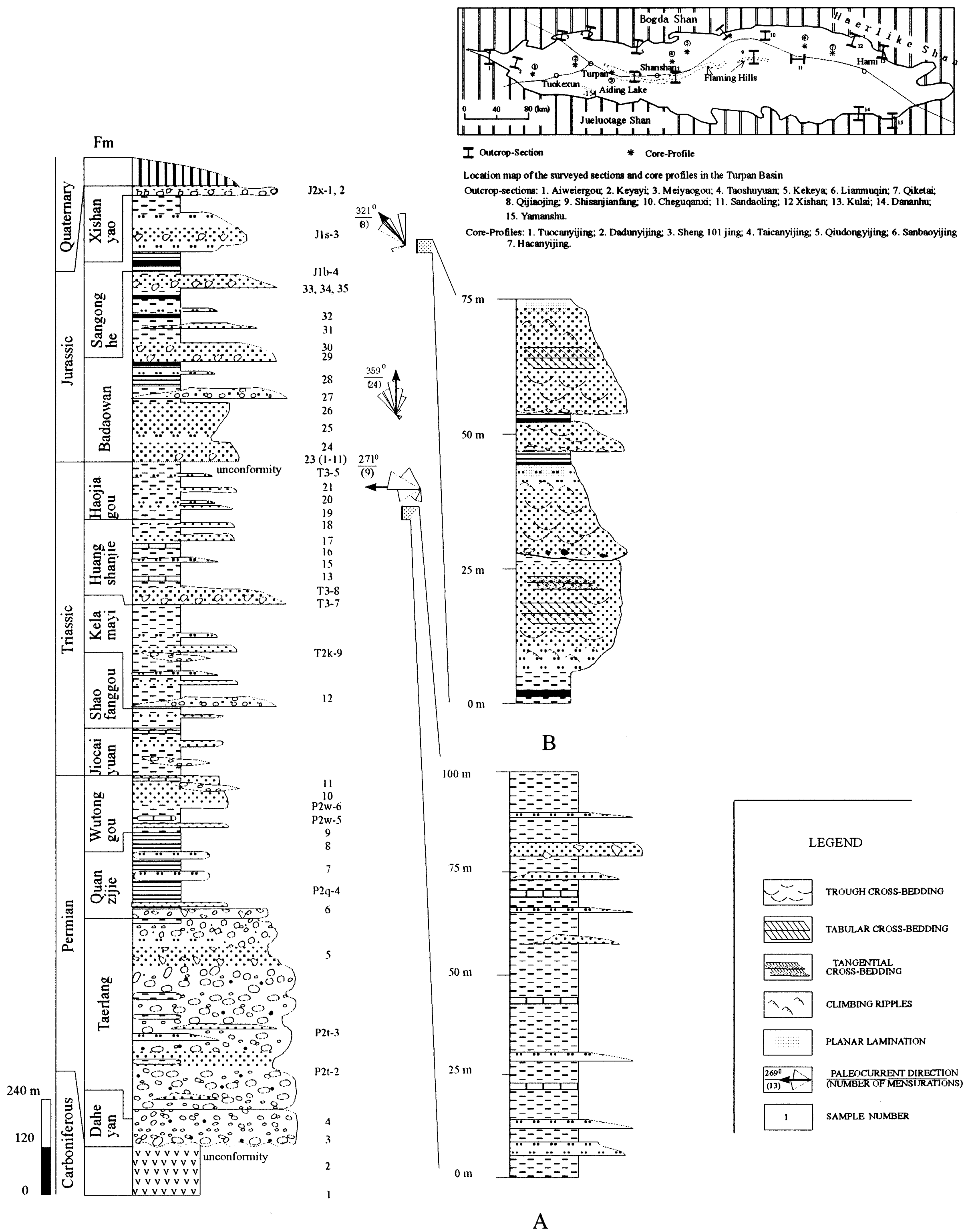

Bogda Shan
Haerlike Shan
Turpan
Tuokexun
Shanshan
Flaming Hills
Aiding Lake
Hami
Jueluotage Shan
0 40 80 (km)
Outcrop-Section
Core-Profile
Location map of the surveyed sections and core profiles in the Turpan Basin
Outcrop-sections: 1. Aiweiergou; 2. Keyayi; 3. Meiyaogou; 4. Taoshuyuan; 5. Kekeya; 6. Lianmuqin; 7. Qiketai; 8. Qijiaojing; 9. Shisanjianfang; 10. Cheguqanxi; 11. Sandaoling; 12 Xishan; 13. Kulai; 14. Dananhu; 15. Yamanshu.
Core-Profiles: 1. Tuocanyijing; 2. Dadunyijing; 3. Sheng 101 jing; 4. Taicanyijing; 5. Qiudongyijing; 6. Sanbaoyijing 7. Hacanyijing.
Fm
Quaternary
Jurassic
Triassic
Permian
Carboniferous
Xishan yao
Sangong he
Badaowan
Haojia gou
Huang shanjie
Kela mayi
Shao fanggou
Jiocai yuan
Wutong gou
Quan zijie
Taerlang
Dahe yan
unconformity
J2x-1, 2
J1s-3
J1b-4
33, 34, 35
32
31
30
29
28
27
26
25
24
23 (1-11)
T3-5
21
20
19
18
17
16
15
13
T3-8
T3-7
T2k-9
12
11
10
P2w-6
P2w-5
9
8
7
P2q-4
6
5
P2t-3
P2t-2
4
3
2
1
321°
(8)
359°
(24)
271°
(9)
240 m
120
0
75 m
50 m
25 m
0 m
B
100 m
75 m
50 m
25 m
0 m
A
LEGEND
TROUGH CROSS-BEDDING
TABULAR CROSS-BEDDING
TANGENTIAL CROSS-BEDDING
CLIMBING RIPPLES
PLANAR LAMINATION
269°
(13)
PALEOCURRENT DIRECTION (NUMBER OF MENSURATIONS)
1
SAMPLE NUMBER

In the eastern part of the basin, the transport direction was from northwest to southeast (Lin, 1993). In the southern part of the basin no sediments were received.

The boundary between the Permian and Triassic west of the Taoshuyuan–Tuokexun line is an angular unconformity. Generally, the Triassic strata consist of red conglomerate, coarse sandstone and sandstone in the lower part and dark, fine clastic sediments with coal and coal streaks in the upper part, deposited in alluvial and lacustrine–fluvial environments and suggesting a process of climate change from arid to humid during the Triassic. The transport directions are shown in Fig. 5. Middle and Late Triassic strata have more variable sediment transport directions than Lower Triassic strata. On the margin of the basin (e.g. Aiweiergou and Taoshuyuan), there are alluvial and braided-fluvial deposits. At Aiweiergou, the transport direction of the sediments was from southwest to northeast. The average of the paleocurrent directions in the Middle Triassic is 271° at Taoshuyuan but 112° at Kekeya (Fig. 5A), suggesting that there was an uplifted region between them.

The Lower and Middle Jurassic strata consist of gray and green clasts and coal deposited in a lacustrine-swamp environment. The Upper Jurassic consists of variegated coarse clastic rocks, deposited in a piedmont–fluvial environment with an arid climate (Li, 1997a; Li, 1997b). In the Early Jurassic, transport directions in the Hami Sag were from northwest to southeast (Fig. 5B). In the Turpan Sag, the paleocurrent directions show that the Bogda Shan was a sedimentary depocenter, and contains Lower and Middle Jurassic fluvial to lacustrine strata with coal. North of Aiweiergou was an uplifted area, which provided the neighboring areas with rock fragments.

In the Middle Jurassic, the eastern part of the Junggar Basin, called the Qitai Paleouplift (Zai, 1993), was joined with the eastern part of the Bogda Shan and denuded (Lin, 1993; Liu and Di, 1997), while the western part of the Bogda Shan received sediments and coal. In the Xishanyao Formation, the paleocurrent directions in most measured sections were from north to south in a range from 188° at Shanshan to 193° at Aiweiergou (Fig. 5C). The Sanjianfang and Qiketai formations are exposed in the middle (Flaming Hills) and at the northern and western margins of the basin. In the middle of the basin, the clast size fines upward from south to north. The paleocurrent analysis shows that the sedimentary transport directions were mostly from south to north (Fig. 5C). In the northeastern part of the Turpan Sag, there are some fan-deltas in the Qiketai Formation, and the sediments came from a nearby source area (Liu et al., 1998).

In the Late Jurassic, the sedimentary rocks are mostly red and purple-red, indicating the paleoclimate changed from humid to arid. At Lianmuqin, the gray-green silty mudstone was deposited in a lacustrine environment, and the paleocurrent directions were from south to north (Fig. 5C). In the latest Jurassic, the Kalaza Formation is less exposed. From north to south, the thickness of the Kalaza Formation decreases and the clast size fines upward. On the northern margin of the basin are numerous alluvial conglomerate deposits. Therefore, the transport direction should be from north to south for the Kalaza Formation.

The boundary between Jurassic and Cretaceous is angular unconformable or non-angular unconformable, and the area of Cretaceous deposition was more limited than in the Jurassic. Cretaceous strata are mostly exposed in the northern and middle parts of the basin. The sedimentary environment belongs to a lacustrine system. The thickness decreases from north to south and the clast size fines, suggesting that the sedimentary transport directions were from north to south.

The Tertiary strata are distributed across the entire basin. The coarse clastic sediments, dominant in the lower part of the strata, were deposited in braided fluvial/alluvial environments, while the fine clasts, dominant in the upper part of the strata, are lacustrine deposits. The depositional environment was locally a salt-water lake within an arid paleoclimate. The basin locally deposited evaporates. The dominant sedimentary transport directions were also from north to south.

Fig. 3. Stratigraphic plots of Taoshuyuan section, including two more detailed corresponding profiles, Northern Turpan Basin. On top showing also the locations of the fifteen surveyed outcrop-sections and seven core-profiles.

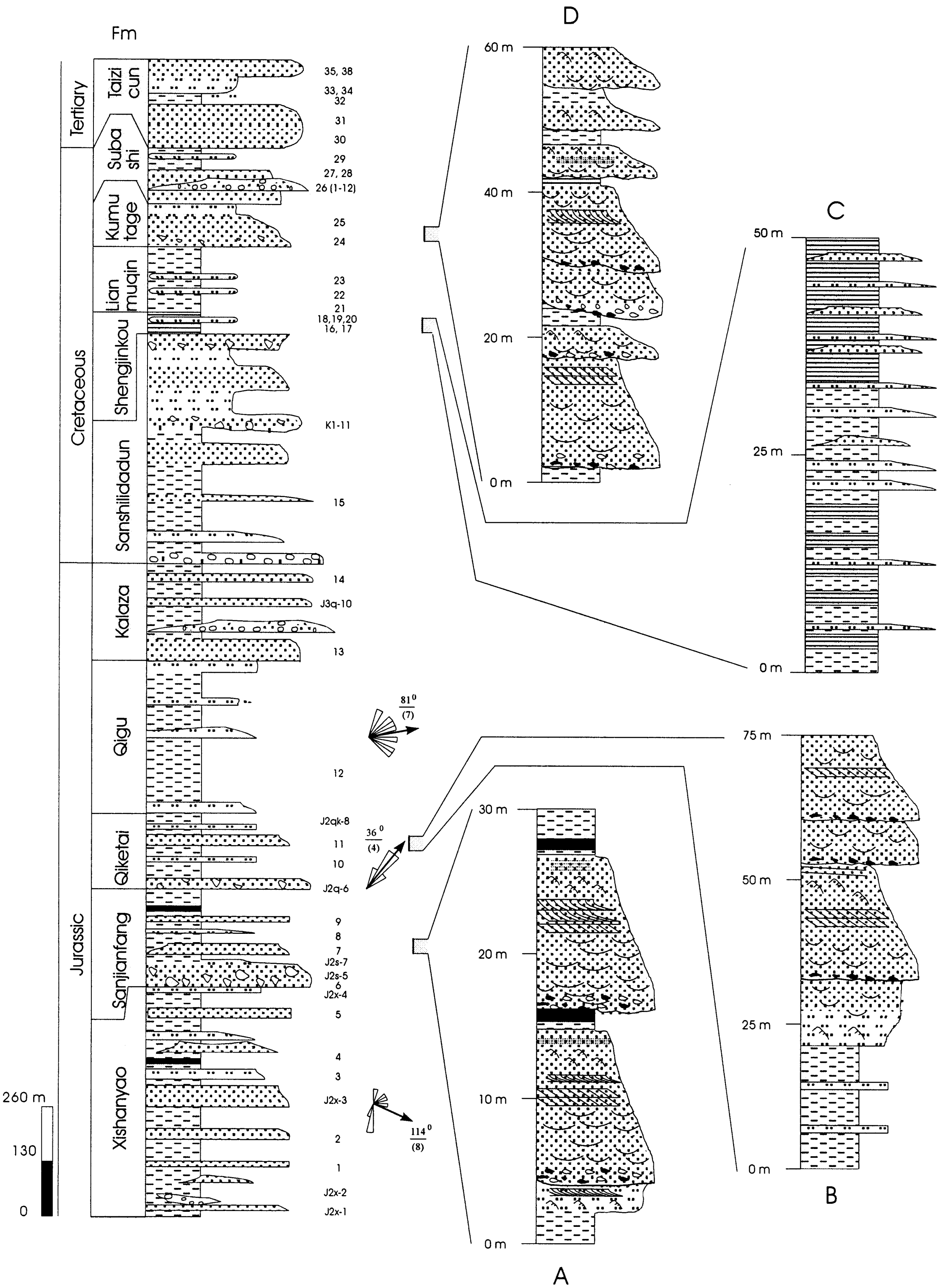

Fm
Tertiary
Cretaceous
Jurassic
Taizi cun
Suba shi
Kumu tage
Lian muqin
Shengjinkou
Sanshilidadun
Kalaza
Qigu
Qiketai
Sanjianfang
Xishanyao
35, 38
33, 34
32
31
30
29
27, 28
26 (1-12)
25
24
23
22
21
18,19,20
16, 17
K1-11
15
14
J3q-10
13
12
J2qk-8
11
10
J2q-6
9
8
7
J2s-7
J2s-5
6
J2x-4
5
4
3
J2x-3
2
1
J2x-2
J2x-1
260 m
130
0
81°
(7)
36°
(4)
114°
(8)
D
60 m
40 m
20 m
0 m
C
50 m
25 m
0 m
75 m
50 m
25 m
0 m
B
30 m
20 m
10 m
0 m
A

6. Subsidence history and basin evolution

The important data of the subsidence analysis are listed in Table 1 and the graphic results are shown in Fig. 6.

Fig. 6 includes curves of total subsidence, tectonic subsidence and paleo-elevation. The total subsidence is more than ten thousand meters from the Early Permian to Miocene in the Turpan Basin. The subsidence diagrams show that the highest rates of subsidence in the Turpan Basin were present throughout the Late Permian and Early Triassic periods, active tectonic subsidence throughout the Middle Triassic and Jurassic, relatively reduced activity during the Cretaceous, and increased activity in the early Tertiary. In addition, periods of accelerated basin subsidence occurred during the Late Permian and Early Triassic, Late Triassic/Early Jurassic, latest Jurassic/earliest Cretaceous, and latest Cretaceous/early Cenozoic. Acceleration of subsidence rates in the Late Permian and Early Triassic was remarkably high. In general, high rates of subsidence coincide with peaks in coarse clastic deposition and there are commonly unconformities before these periodic high rates of subsidence (Fig. 6). The subsidence rate in the Jurassic is also obviously high; however, sedimentation of the Lianmuqin section contains only a small amount of coarse clastic deposits. In this period, the strata formed at the southern margin of the basin contain more coarse clastic deposits. For instance, the Upper Jurassic at the Aiweiergou section consists almost entirely of conglomerate, while there is only fine sedimentation in the Lianmuqin section. The coarse clastic deposition did not prograde far enough basinward to the middle part of the basin in the Jurassic.

Volcanic and intrusive activities were quite extensively developed in the Turpan Basin region during the Carboniferous and Early Permian, but ceased following Late Permian time. The curves of basin subsidence from the Late Permian to Early Triassic are strongly concave-up, forming the highest subsidence rate of the basin. Mckenzie (1978) suggested that the greatest subsidence of theoretical models of thermal subsidence occurs within about 50 Ma after the onset of extension. This situation was present also in the Turpan Basin. These segments of the curves are interpreted to reflect thermal subsidence following the period of magmatic activities in this region, and mark the beginning of the evolution of the basin. In this period, the Turpan Basin was extended (Tao, 1994), rapidly subsided and received a large amount of coarse clastic sediments. The typical thermal subsidence curve should be strongly concave-up at first and then flatten (Angevine et al., 1990), and the curve is general continuous. However, there is an acceleration in the curve in the Late Permian or Early Triassic. At this time, the Tarim Block was transported towards the north and collided with the Eurasia Plate (Zhang and Wu, 1985; Lin, 1985; Cheng et al., 1986; Zhou et al., 1996). This tectonic event disturbed the thermal subsidence curve of the basin.

During the Middle Triassic and early Tertiary, the total subsidence rate of the basin was generally high (ca. 29 m/Ma), although the tectonic subsidence rate is considerably less than before. There were several periods of accelerated subsidence typical of flexural loading subsidence during these times. Accelerated subsidence occurred during the Late Triassic/Early Jurassic, latest Jurassic/earliest Cretaceous, and latest Cretaceous/early Cenozoic, induced by several advancing thrust sheets during crustal shortening and orogenic movements. During these times, the Qiangtang Block, the Gangdise Block and the Indian Subcontinent collided and converged with the Eurasian Plate (Liu et al., 1990). Moreover, Liu et al. (1990) pointed out that the Gangdise Block collided with the Eurasian in the Late Jurassic, but separated from it shortly thereafter. In the latest Jurassic/earliest Cretaceous they collided again. The subsidence rates of the basin are generally high from the Middle Triassic to Jurassic, indicating an important period of subsidence for the basin. It is remarkable that both total and tectonic subsidence rates are clearly reduced during the Cretaceous. The convergence of the Gangdise Block may have decreased the subsidence rates for the entire basin and produced the unconformity between Jurassic and Cretaceous strata. Due to

Fig. 4. Stratigraphic plots of the Lianmuqin section, including four more detailed corresponding profiles, middle of Turpan Basin. For legend see Figs. 2 and 3.

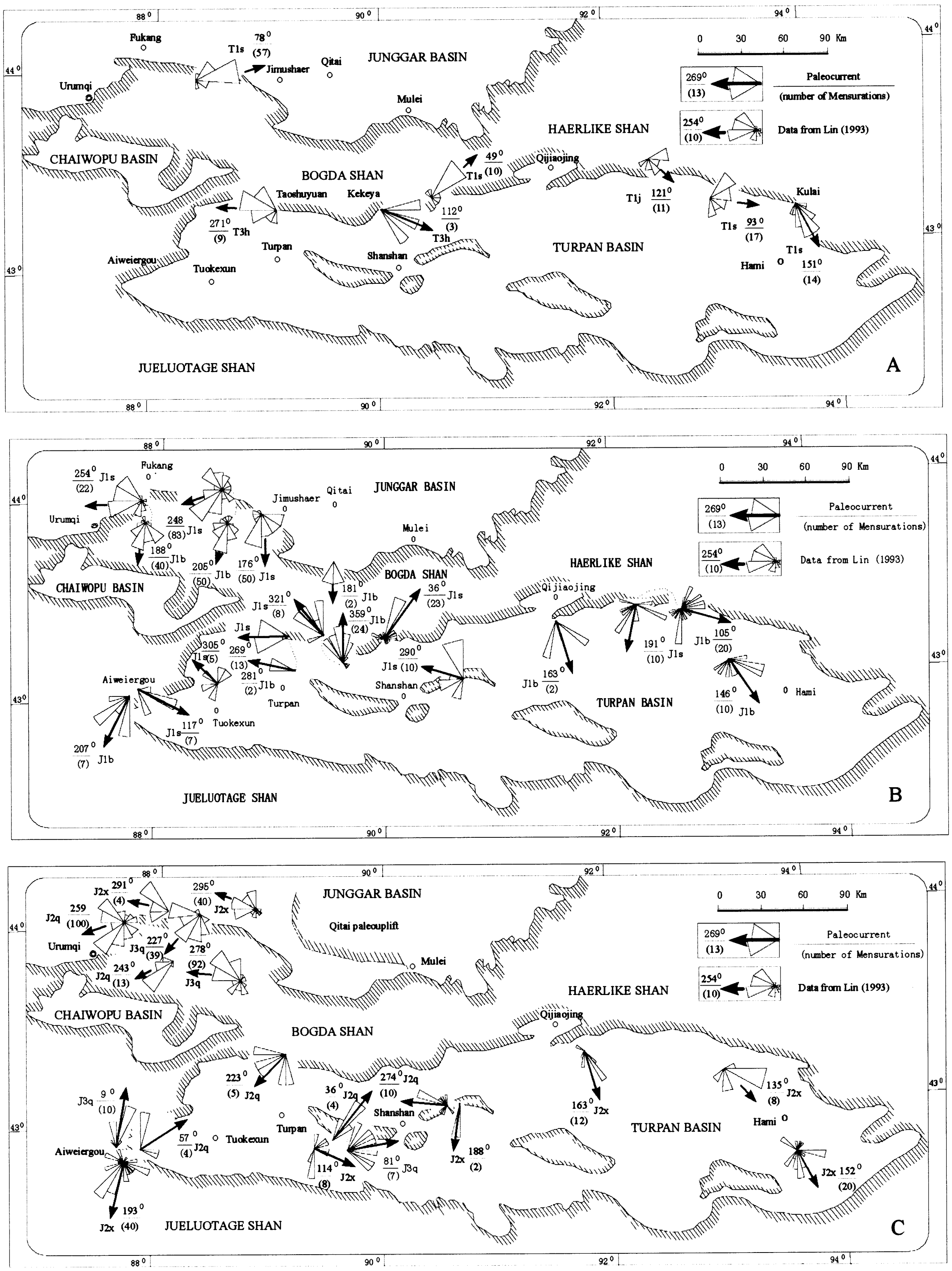
JUNGGAR BASIN
0 30 60 90 Km
Paleocurrent
(number of Mensurations)
Data from Lin (1993)
Fukang
Urumqi
Jimushaer
Qitai
Mulei
HAERLIKE SHAN
CHAIWOPU BASIN
BOGDA SHAN
Taoshuyuan
Kekeya
Qijiaojing
Kulai
Turpan
Shanshan
Aiweiergou
Tuokexun
TURPAN BASIN
Hami
JUELUOTAGE SHAN
A
B
Qitai paleouplift
C
88°
90°
92°
94°
43°
44°

Table 1
Data list for the subsidence analysis of the Turpan Basin (density after Allen and Allen, 1990)

Period (Ma)	Series	Groups	Formations	Thickness (m)	Depth (m)	Φ_0	C (km^{-1})	P_{sg} ($kg\ m^{-3}$)
					0			
	Miocene		Putaoyuan	901	901	0.46	0.43	2695
23 Tertiary	Oligocene		Taoshuyuan	1117	2018	0.47	0.44	2694
	Eocene	Shanshan	Bakaner	258	2276	0.49	0.49	2713
56	Paleocene		Taizichun	95	2371	0.40	0.31	2644
65	Upper Cretaceous		Subashi	133	2504	0.43	0.36	2672
			Kumutage	96	2600	0.40	0.27	2650
97	Lower Cretaceous	Tugulu	Lianmuqin	163	2763	0.48	0.46	2706
Cretaceous			Shengjinkou	55	2818	0.48	0.45	2703
			Sanshilidadun	534	3352	0.45	0.39	2684
145.6	Upper Jurassic	Aiweiergou	Kalaza	218	3570	0.44	0.38	2678
			Qigu	355	3925	0.49	0.49	2713
157	Middle Jurassic		Qiketai	177	4102	0.47	0.44	2694
Jurassic			Sanjianfang	350	4452	0.47	0.44	2698
		Shuixigou	Xishanyao	530	4982	0.45	0.39	2684
178	Lower Jurassic		Sangonghe	194	5176	0.43	0.36	2668
			Badaowan	490	5666	0.43	0.37	2593
208	Upper Triassic	Xiaoquangou	Haojiagou	159	5825	0.48	0.47	2709
			Huangshanjie	217	6042	0.48	0.47	2707
235 Triassic	MiddleTriassic		Kelamayi	283	6325	0.48	0.47	2705
241	Lower Triassic	Upper Cangfanggou	Shaofanggou	47	6372	0.49	0.49	2711
			Jiocaiyuan	132	6504	0.48	0.47	2707
245	Upper Permian	Lower Cangfanggou	Wutonggou	288	6792	0.45	0.41	2685
			Quanzijie	214	7006	0.44	0.38	2679
Permian		Taodonggou	Taerlang	514	7520	0.38	0.27	2628
			Daheyan	69	7589	0.35	0.25	2603
256	Lower Permian		P1	?	?			

～～～ or .... angular or parallel unconformity.
Φ_0 surface porosity. C: depth coefficient. P_{sg}: density (Allen and Allen, 1990).

the collision between the Indian and Eurasian plates in the Cenozoic, the Bogda Shan was strongly folded and uplifted, providing considerable detritus to the basin, and leading to renewed subsidence. Therefore, these accelerated subsidence periods reflect clearly a complex and polycyclic tectonic history in the evolution of the basin and surrounding areas (Fig. 7).

Hendrix et al. (1992) displayed a subsidence his-

Fig. 5. Plots of paleocurrent directions of the Turpan Basin. (A) Triassic (*T1j* = Jiocaiyuan Formation; *T1s* = Shaofanggou Formation; *T3h* = Haojiagou Formation). (B) Lower Jurassic (*J1b* = Badaowan Formation; *J1s* = Sangonghe Formation). (C) Middle and Upper Jurassic (*J2x* = Xishanyao Formation; *J2q* = Qiketai Formation; *J3q* = Qigu Formation).

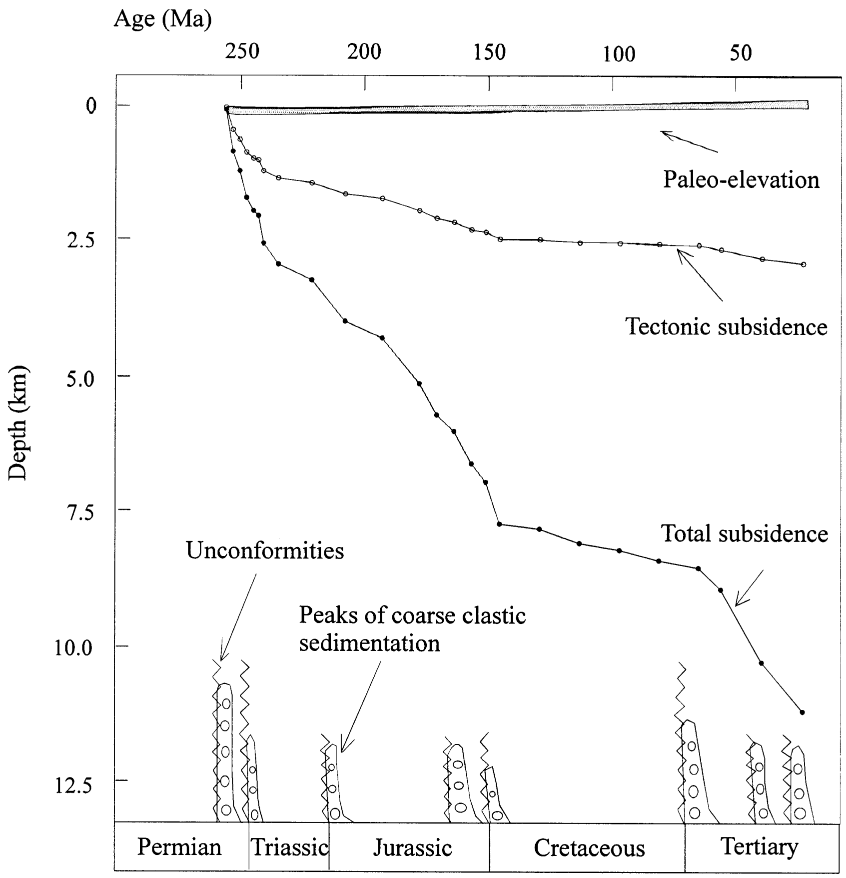

Fig. 6. Subsidence history diagrams for the Turpan Basin, displaying that the Turpan Basin underwent first thermal subsidence and then flexure subsidence. The thermal subsidence took place during the Upper Permian and Early Triassic. The flexure subsidence was throughout the Middle Triassic to Early Tertiary. There are several accelerated subsidence periods associated with the alluvial coarse clastic sediments commonly overlying major unconformities.

tory diagram of the Turpan Basin. Their subsidence diagrams show that the higher rates of subsidence occurred shortly after coarse clastic deposition. However, this situation did not appear in our study. According to the diagram (Fig. 6) and detailed field observations, the higher rates of basin subsidence occurred with coarse clastic deposition at the same time, reflecting a coincidence of the rapid tectonic subsidence and the strong erosion in the nearby source regions.

7. Concluding remarks

Late Paleozoic through Cenozoic sedimentary environments in the Turpan Basin changed with time. In the Permian, the sedimentary environment shifted from marine to continental facies. In the Mesozoic and Cenozoic, the Turpan Basin was entirely nonmarine. The sedimentary environments included alluvial, fluvial and lacustrine strata. The paleoclimate changed from arid to humid during the Triassic, and from humid to arid from the Jurassic to Cretaceous. In Tertiary times, the Turpan Basin locally developed evaporates.

Along with the tectonic variation, the paleocurrent indicator directions of the basin varied also with time. From Permian to Jurassic times, the Jueluotage Shan was the dominant source rock region for the Turpan Basin. The locally uplifted areas of the Bogda Shan (e.g. at Taoshuyuan) were only minor providers of source rocks. The paleocurrent direc-

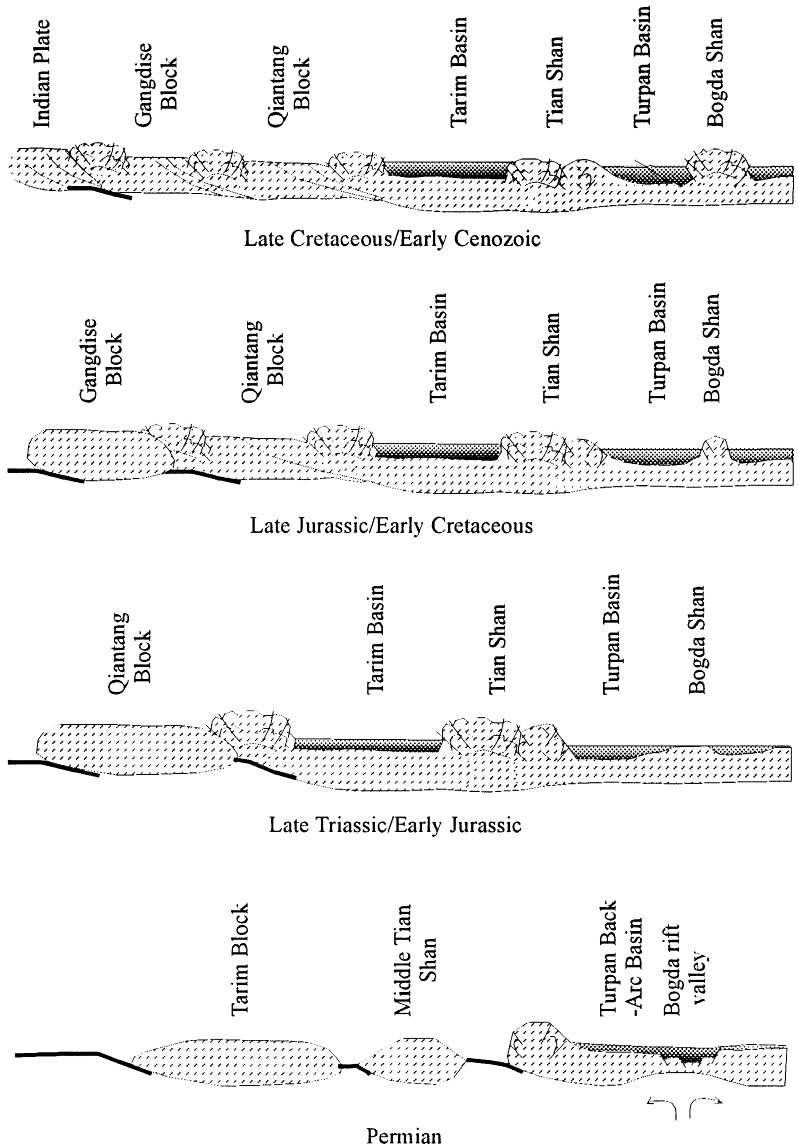

Fig. 7. Cross-sections showing the tectonic evolution of the Turpan Basin and adjacent areas.

tions were from south to north. The Qitai paleouplift was an important provenance area for the northern region of the basin. Since the latest Jurassic, the Bogda Shan was gradually folded and uplifted, building another source rock region for the basin. The paleocurrent directions were from north to south. In the Cretaceous and Tertiary, the Bogda Shan was an important source rock region. This region was continually strongly uplifted in Cenozoic time and the dominant source rock region for the basin. In the Hami Sag, the Haerlike Shan was a continuously eroding region and always an important source area. The paleocurrent directions were always from north to south.

The Turpan Basin formed during the Late Permian and underwent first thermal subsidence and then flexural subsidence. The evolution of the basin can be divided into four periods: the rapidly subsiding period (from the Late Permian to Early Triassic); the actively subsiding period (from the Middle Triassic to Jurassic), reduced subsiding period (Cretaceous) and increased subsiding period (early Tertiary). The thermal subsidence took place during the Late Permian and Early Triassic following the period of plate collision and magmatic activities in this region. Convergence between the Tarim Block and the Eurasian Plate during the Late Permian/Early Triassic appears to be reflected by a temporary increase in subsidence. Due to the thermal subsidence and tensile situation, it may have been a back-arc basin in the late Paleozoic. Flexural subsidence throughout the Middle Triassic to Early Tertiary was induced by several collisions which produced periods of high subsidence rates during the Late Triassic/Early Jurassic, latest Jurassic/earliest Cretaceous, and latest Cretaceous/early Cenozoic. We interpret these periods of accelerated subsidence to reflect accretion onto the south Asian continental margin of the Qiangtang Block in the Late Triassic/Early Jurassic, the Gangdise Block in latest Jurassic/earliest Cretaceous, and the Indian Subcontinent in the latest Cretaceous/early Cenozoic.

Acknowledgements

Thanks to Prof. Zhou Lifa and Dr. Lin Jinyan, Northwest University, Xi'an who supported our field work. The authors also wish to acknowledge financial assistance partly from the Postdoctoral Science Foundation of China and the Bureau of Personnel of Shanghai Government.

References

Allen, M.B., Windley, B.F., 1993. Evolution of the Turfan Basin, Chinese Central Asia. Tectonics 12, 889–896.

Allen, P.A., Allen, J.R., 1990. Basin Analysis. Blackwell, Oxford, 443 pp.

Angevine, Ch.L., Heller, P.L., Paola, C., 1990. Quantitative Sedimentary Basin Modeling. Am. Assoc. Pet. Geol. Bookstore, 132 pp.

Bally, A.W., Chou, I.M., Clayton, R., Eugster, H.P., Kidwell, S., Meckel, L.D., Ryder, R.T., Watts, A.B., Wilson, A.A., 1986. Notes on sedimentary basins delegation to the People's Republic of China. U.S. Geol. Surv. Open-File Rep. 86-327, 108 pp.

Bureau of Geology and Mineral Resources of Xinjiang Uygur Autonomous Region, 1966. 1 : 200,000 Geologic maps of Turpan Basin, Xinjiang Uygur Autonomous Region, China. Geological Publishing House, Beijing.

Bureau of Geology and Mineral Resources of Xinjiang Uygur Autonomous Region, 1991. Paleozoic of Xinjiang, B. 343–360, Urumqi (in Chinese). Xinjiang People's Publishing House, 482 pp.

Cao, C.Z., 1990. The plate tectonic of northern Xinjiang, northwest China (in Chinese). Bull. Shenyang Inst. Geol. Miner. Resour., Chin. Acad. Geol. Sci. 22, 26–32.

Carroll, A.R., Liang, Y.H., Graham, S.A., Xiao, X.C., Hendrix, M.S., Chu, J.C., Mcknight, C.L., 1990. Junggar basin, northwest China, trapped late Paleozoic ocean. Tectonophysics 181, 1–14.

Carroll, A.R., Graham, S.A., Hendrix, M.S., Chu, J.C., McKnight, C.L., Feng, Y.M., Liang, Y.H., Xiao, X.C., Zhao, M., Tang, Y.Q., Li, J.Y., Zhu, B.Q., 1991. Characteristics of sedimentation in Late Paleozoic Junggar Basin and its basement. In: Xiao, X.C., Tang, Y.Q. (Eds.), On Tectonic Evolution of the Southern Margin of the Paleoasian Composite Megasuture Zone. Beijing Science and Technic Publishing House, Beijing, pp. 136–150.

Chen, Z.F. (Ed.), 1985a. 1 : 2,000,000 Geologic Map of Xinjiang Uygur Autonomous Region, China. Geological Publishing House, Beijing.

Chen, Z.F. (Ed.), 1985b. Explanatory Notes on the Geological Map of Xinjiang Uygur Autonomous Region, China (in Chinese with English abstract). Geological Publishing House, Beijing.

Cheng, S.D., Wang, G.R., Yang, S.D., Jing, J.S., Zhu, J.S., 1986. The paleoplate tectonic of Xinjiang (in Chinese with English abstract). Xinjiang Geol. 4, 1–26.

Harland, W.B., Armstrong, R.L., Cox, A.V., Craig, L.E., Smith, A.G., Smith, D.G., 1990. A Geologic Time Scale 1989. Cambridge University Press, New Youk, 263 pp.

He, G.Q., Li, M.S., Liu, D.Q., Tang, Y.L., Zhou, R.H., 1994. Paleozoic Crustal Evolution and Mineralization in Xinjiang of China (in Chinese with English abstract). Xinjiang People's Publishing House, 437 pp.

Hendrix, M.S., Graham, S.A., Carroll, A.R., Sobel, E.R., McKnight, C.L., Schulein, B.J., Wang, Z.X., 1992. Sedimentary record and climatic implications of recurrent deformation in the Tian Shan: evidence from Mesozoic strata of the north Tarim, south Junggar, and Turpan basin, northwest China. Geol. Soc. Am. Bull. 104, 53–79.

Hu, J.Y., Zhao, W.Z., Qian, K., Li, X.D., Li, Q.M., 1996. Fundamental characteristics of petroleum geology in NW China (in Chinese with English abstract). Acta Pet. Sin. 17, 1–11.

Huang, J.Q., 1978. An outline of the tectonic characteristics of China. Eclogae Geol. Helv. 71, 611–635.

Jin, H.J., 1989. Trace fossils in Late Paleozoic deep-water sediments of Junggar Basin, and its significance in the environment (in Chinese with English abstract). Acta Sedimentol. Sin. 7, 23–40.

Jin, H.J., Li, Y.C., 1989. Tempestite-Bathya mass gravitative transported deposit in Late Paleozoic and its formation tectonic background in southwestern Bogda Mountain (in Chinese with English abstract). Acta Sedimentol. Sin. 7, 7–22.

Li, W.H., 1997a. Sequence stratigraphy of Jurassic in Taibei Sag, Turpan-Hami Basin (in Chinese with English abstract). Oil Gas Geol. 3 (18), 210–215.

Li, W.H., 1997b. Wenjisang braid delta in Taibei Sag, Turpan-Hami Basin and its hydrocarbon accumulation (in Chinese with English abstract). Oil Gas Geol. 3 (18), 231–235.

Lin, J.L., 1985. APW paths for the North and South China blocks. Seismol. Geol. 7, 81–83.

Lin, J.Y., 1993. Sedimentary sequence of the Bogda Rift: Discussion about the Formation and Evolution of the Entire Intercontinental Sedimentary Basin in the Northern Xingjiang (in Chinese). Ph.D. thesis, Northwest University, Xi'an, 104 pp.

Liu, L.Y., Di, S.X., 1997. Characteristics of middle Jurassic sedimentation and reservoir pore evolution in Turpan Depression (in Chinese with English abstract). Oil Gas Geol. 3 (18), 247–260.

Liu, L.Y., Liu, Y.Q., Di, S.X., 1998. Sedimentation and diagenesis of Qiketai formation in north Turpan Depression (in Chinese with English abstract). Oil Gas Geol. 3 (19), 238–243.

Liu, Z.Q., Xu, X., Pan, G.T., Li, T.J., Yu, G.M., Yu, X.J., Jiang, X.Z., Wei, G.Y., Wang, C.S., 1990. Tectonics, geological evolution and genetic mechanism of Qinghai–Xizang Plateau (in Chinese with English abstract). People's Republic of China, Ministry of Geology and Mineral Resources, Geological Memoirs, series 5 (10). Geology Press, Beijing, pp. 106–127.

Mckenzie, D.P., 1978. Some remarks on the development of sedimentary basin. Earth Planet. Sci. Lett. 40. 25–32.

Miall, A.D., 1990. Principles of Sedimentary Basin Analysis (2nd ed.). Springer, Berlin, 668 pp.

Peng, Z.L., Zheng, J.J., Huang, H.F., Liu, Z.G., 1995. Classification of the chief sedimentary basins in China (in Chinese with English abstract). Acta Sedimentol. Sin. 13, 150–159.

Potter, P.E., Pettijohn, F.J., 1963. Paleocurrents and Basin Analysis. Springer, Berlin, 296 pp.

Ren, J.S., Jiang, C.F., Chang, Z.Q., Chin, D.Y., 1980. The Geotectonic Evolution of China (in Chinese). Science Publishing House, Beijing, 124 pp.

Shao, L., 1996. Sedimentology and Evolution of the Turpan Basin (NW China): Institute Report of Geologic and Paleontologic Institute. Kiel University Press, Germany, no. 80, pp. 102–106.

Shao, L., Li, W.H., Yuan, M.S., 1999. Characteristic of sandstone and its tectonic implications of the Turpan Basin (in Chinese with English abstract). Acta Sedimentol. Sin. 1 (17), 95–99.

Song, C.H., Jin, H.J., 1989. The evolution and sediment types of debris flow and high-density turbidity current of Shirenzigou Formation, the Lower Permian in Sangonghe area, Northern Piedmont of the Bogda Mountain (in Chinese with English abstract). Acta Sedimentol. Sin. 7, 95–107.

Steckler, M.S., Watts, A.B., 1978. Subsidence of the atlantic-type continental margin off New York. Earth Planet. Sci. Lett. 41, 1–13.

Tang, Y.Q., Zhao, M., 1991. Plate tectonic evolution of the Tianshan, China. In: Xiao, X.C., Tang, Y.Q. (Eds.). On Tectonic Evolution of the Southern Margin of the Paleoasian Composite Megasuture Zone. Beijing Science and Technic Publishing House, Beijing, pp. 109–124.

Tao, M.X., 1994. Tectonic environmental analysis of Turpan–Hami Basin. On the genetic relationship between basin and orogenic belt of continental inner plate (in Chinese with English abstract). Acta Sedimentol. Sin. 12, 40–50.

van Hinte, J.E., 1978. Geohistory — application of micropaleontology in exploration geology. Am. Assoc. Pet. Geol. 62, 201–222.

Wu, Q.F., 1986. Tectonic evolution and petroleum potential of the Junggar basin (in Chinese with English abstract). Xinjiang Geol. 4, 1–19.

Wu, T., Zhao, W.Z., 1997. The Formation and Distribution of Coal-Bearing Oil Fields in Turpan Basin (in Chinese). Petroleum Industry Publishing House, Beijing, 271 pp.

Wu, T., Yuan, M.S., Wang, W.H., 1992. Tectonic evolution and petroleum accumulation of the Turpan Basin (in Chinese with English abstract). Pet. Geol. 9, 165–174.

Wu, T., Zhang, S.H., Wang, W.H., 1996. The structural characteristics and hydrocarbon accumulation in Turpan–Hami coal-bearing basin (in Chinese with English abstract). Acta Pet. Sin. 17, 12–18.

Wu, Z.Z., 1986. A discussion on platetectonic evolution, distribution and petroleum potential of the Junggar Basin (in Chinese with English abstract). Xinjiang Geol. 4, 20–34.

Xiao, X.C., Tang, Y.Q., Feng, L.M., Zhou, B.Q., Li, Q.T., Zhao, M., 1992. Tectonic Evolution of the Northern Xinjiang and Adjacent Regions (in Chinese with English abstract). Geological Publishing House, Beijing, 169 pp.

Zai, G.M. (Ed.), 1993. Petroleum Geology of China, vol. 15: Part II. Junggar Basin, Stratigraphy and Sedimentary Facies (in Chinese). Petroleum Industry Publishing House, Beijing, pp. 57–98.

Zhang, L., 1983. On the age of Badaowan Formation in northern Xinjiang. Sci. Sin. (Ser. B) 26, 313–323.

Zhang, L.C., Wu, N.Y., 1985. The geotectonic and its evolution of the Tian Shan (in Chinese with English abstract). Xinjiang Geol. 3, 1–14.

Zhang, X., 1981. Regional Stratigraphic Chart of Northwestern China, Branch of Xinjiang Uygur Autonomous Region (in Chinese). Geological Publishing House, Beijing, 496 pp.

Zhao, W.Z., Yuan, F., Zeng, X.M., 1992. The structural characteristics of Turpan–Harmy Basin (in Chinese with English abstract). Acta Pet. Sin. 3 (13), 9–17.

Zhou, J.Y., Zhang, B., Zhang, C.W., Wei, G.Y., Lu, Y., Xia, J., Cui, B.F., Wang, C.Y., Li, B.H., 1996. Geology of the Silver, Rhenium–Molybdenum, Gold and Copper Deposits in the Eastern Tianshan and its Adjacent Regions (in Chinese with English abstract). Geological Publishing House, Beijing, 191 pp.

Zhu, X., Chen, H.J., 1980. On the tectonic evolution of Chinese petroleum basin (in Chinese with English abstract). In: Scientific Papers on Geology for International Exchange. Geological Publishing House, Beijing, pp. 263–267.

Zhu, X., Yang, H., 1988. Evolutionary characteristics of intermontane coal basins of the Mesozoic and Cenozoic basins in Tianshan (in Chinese with English abstract). Xinjiang Geol. 6, 83–91.